Cancer Control
Volume 26: 1-10
© The Author(s) 2019
Article reuse guidelines:
sagepub.com/journals-permissions
DOI: 10.1177/1073274819865281
journals.sagepub.com/home/ccx
SAGE

The Value of CT and MRI for Determining Thymoma in Patients With Myasthenia Gravis

Phung Anh Tuan, MD, PhD[1], Mai Van Vien, MD, PhD[1], Hoang Van Dong, MD, PhD[2], David Sibell, MD, PhD[3], and Bui Van Giang, MD, PhD[2]

Abstract

The aim of the study was to evaluate the usefulness of computed tomography (CT) and magnetic resonance imaging (MRI) for differentiating thymoma from nonthymoma abnormalities in patients with myasthenia gravis (MG). A cross-sectional study of 53 patients with MG, who had undergone surgical thymectomy, was conducted at 103 Hospital (Hanoi, Vietnam) and Cho Ray Hospital (Ho Chi Minh City, Vietnam) during August 2014 and January 2017. The CT and MRI images of patients with MG were qualitatively and quantitatively (radiodensity and chemical shift ratio [CSR]) analyzed to determine and compare their ability to distinguish thymoma from nonthymoma abnormalities. Logistic regression was used to identify the association between imaging parameters (eg, CSR) and the thymoma status. The receiver operating curve (ROC) analysis was used to determine the differentiating ability of CSR and radiodensity. As results, of the 53 patients with MG, 33 were with thymoma and 20 were with nonthymoma abnormalities. At qualitative assessment, MRI had significantly higher accuracy than did CT in differentiating thymoma from nonthymoma abnormalities (94.3% vs 83%). At quantitative assessment, both the radiodensity and CSR were significantly higher for thymoma compared with nonthymoma groups ($P < .001$). The ROC analysis showed that CSR had significantly higher sensitivity (Se) and specificity (Sp) than radiodensity in discriminating between the 2 groups (CSR: Se 100%, Sp 95% vs radiodensity: Se 90.9%, Sp 70%). When combining both qualitative and quantitative parameters, MRI had even higher accuracy than did CT in thymoma diagnosis ($P = .031$). In conclusion, chemical shift MRI was more accurate than CT for differentiating thymoma from nonthymoma in patients with MG.

Keywords

thymoma, myasthenia gravis, MRI, CT, CSR

Received March 10, 2019. Received revised June 18, 2019. Accepted for publication June 28, 2019.

Introduction

Myasthenia gravis (MG) is a relatively uncommon disease. The thymus plays an important role in the pathogenesis of MG. Approximately 90% of patients with MG displayed thymic abnormalities, such as hyperplasia (70%) and thymoma (20%).[1] The differentiation of thymoma from thymic lymphoid hyperplasia is critical in the evaluation for surgical treatment. Thymectomy is strongly recommended in all thymoma cases,

[1] 103 Hospital, Ha Dong, Hanoi, Vietnam
[2] National Cancer Hospital, Ha Dong, Hanoi, Vietnam
[3] Oregon Health & Science University, Portland, OR, USA

Corresponding Author:
Bui Van Giang, National Cancer Hospital, 30 Cau Buou, Ha Dong, Hanoi, Vietnam.
Email: buivangiang@hmu.edu.vn

whereas the surgical indication in hyperplasia cases should be only considered when conservative treatments are ineffective. The anatomical distinction is based on morphological assessments on computed tomography (CT). Thymoma is seen as a focal soft tissue mass, whereas thymic hyperplasia shows a diffuse symmetric enlargement gland. However, it is difficult to differentiate the 2 conditions on CT because of high interrater variation. Thymic lymphoid hyperplasia may display as a focal soft tissue mass; in contrast, thymoma may demonstrate diffuse enlargement in both lobes. In these cases, CT results in indeterminate findings, whereas chemical shift magnetic resonance imaging (MRI) may differentiate pathologies by detecting fat in tissue, showing signal intensity (SI) loss on opposed-phase imaging compared to in-phase imaging.[2] In Vietnam, there are very few publications on thymoma as well as on the use of CT and MRI in the diagnosis of this tumor.[3] The aim of this study was to evaluate the usefulness of CT and MRI for differentiating thymoma from nonthymoma abnormalities in patients with MG.

Methods

Participants and Study Design

A cross-sectional study of 53 participants was conducted in Hanoi and Ho Chi Minh City, Vietnam, during August 2014 and January 2017. Participants were patients with MG who had undergone surgical thymectomy at 103 Hospital (Hanoi) and Cho Ray Hospital (Ho Chi Minh City), which are the 2 referral hospitals in Vietnam for the diagnosis and treatment of MG. The inclusion criteria were: (1) new onset of generalized MG, (2) definitive diagnosis based on postresection histological findings, and (3) being naive to neoadjuvant chemoradiotherapeutic treatment. As generalized MG was not a common disease in Vietnam, all eligible patients with MG were consecutively enrolled, except those who were under 16 years.

Data Collection

The information on demographic and clinical characteristics of the patients was extracted from the participants' medical records, while the information on imaging assessment (CT and MRI) of the patients was collected according to the imaging protocols given below. The data collection was performed by 2 experienced radiologists, using a unique protocol, with supervision of the first author of the present manuscript (principle investigator).

Computed tomography examination. Computed tomography examination was carried out using a 2-section CT system (Somatom Spirit; Siemens, Munich, Germany) in a single breath hold at end-inspiration. Technical parameters were set at 120 kVp, 180 mAs, pitch of 1, section thickness of 5 mm, contiguous section interval, and 512 $\times$ 512 matrix without contrast agent intravenous injection. Observation was performed on soft tissue window W350, L100 HU.

Table 1. Thymic MRI Protocol.

Pulse Sequence	TR	TE	Thickness
Axial double IR T1-weighted imaging with CG	1000	10	6
Axial double IR T2-weighted imaging with CG	2000	60	6
Sagittal double IR T2-weighted imaging with CG and fat saturation	2000	60	6
Axial in-phase and opposed-phase T1-weighted fast incoherent gradient-echo imaging	150	4.6; 2.3	5

Abbreviations: CG, cardiac gating; IR, inversion recovery; MRI, magnetic resonance imaging; TE, echo time; TR, recovery time.

Magnetic resonance imaging examination. Magnetic resonance imaging examination was carried out using a 1.5 T MRI unit (Intera; Philips Healthcare, Best, the Netherlands) with phased-array surface coil (Torso coil with 8 channels) from the thoracic inlet to the cardiophrenic angle. All patients underwent transverse gradient-echo T1-weighted in- and opposed-phase imaging using an anterior-to-posterior phase-encoding direction. In 49 patients, dual-echo technique in single breath hold was performed. In 4 patients, non-dual-echo technique in separated breath holds was performed. Axial T1-weighted, T2-weighted and sagittal T2-weighted with fat suppression and black blood technique were added. Imaging parameters are listed in Table 1.

Imaging assessment. Two radiologists, with 20 and 23 years of experience, and without knowledge of patients' diagnosis, independently analyzed the imaging data to retrieve qualitative and quantitative data. In cases of discrepancies, consensus between the 2 radiologists was used to determine the imaging data.

The collected qualitative data were location; shape and position of the gland/tumor; level of necrosis; attenuation; SI on T1-weighted, T2-weighted, and T2-weighted with fat suppression; and SI loss on the opposed-phase relative to the in-phase image. The gland shape was divided into 2 forms: bilateral gland (triangle, arrow) and soft tissue mass. The gland SI on T1-weighted and T2-weighted was divided into 2 levels as equal or higher than muscle but lower than fat and other. Necrotic or cystic component was presumed to be present when an area of low SI was seen on T1-weighted images, and high SI was seen on T2-weighted or Short TI Inversion Recovery images.

The collected quantitative data were the radiodensity, for CT, and chemical shift ratio (CSR), for MRI. In order to measure the radiodensity, region of interest (ROI) was manually drawn at the level where the thymus appeared largest on the cross-sectional image, with exclusion of peripheral areas, calcifications, cystic, or necrotic components as well as beam-hardening artefacts. The SI measurements within the thymus and chest wall muscle were obtained by using ROI (area, 0.5-1 cm^2 for the thymus gland and 1-2 cm^2 for the chest wall muscle), then were used for calculation of CSR. The selection

Table 2. Computed Tomography and Magnetic Resonance Imaging Criteria for Thymoma and Nonthymoma.

Criteria	CT	MRI
Diagnosis of thymoma, at least one of the following:		
Focal soft tissue mass with heterogeneous morphology and irregular shape	Yes	Yes
Nodular lesion with size of nodule ≥1 cm	Yes	Yes
Presence of calcifications and/or cystic/necrotic components regardless of morphology	Yes	Yes
No signal intensity loss on opposed-phase images relative to in-phase images	-	Yes
Diagnosis of nonthymoma, at least one of the following:		
Normal gland thymus shape (triangle, arrowhead) regardless of attenuation and margins	Yes	Yes
Micronodularity (<1 cm) of parenchyma in the anterior mediastinal fat	Yes	Yes
Focal mass with clear entire fat attenuation	Yes	Yes
Homogeneous signal intensity decrease on opposed-phase images relative to in-phase images	-	Yes

Abbreviations: CT, computed tomography; MRI, magnetic resonance imaging.

of the ROI placement was first made on the opposed-phase image, on the area which exhibits the highest SI and then mirrored on the in-phase image in the exact same position and the same size. Measurements were made in the central position and not in peripheral areas to avoid partial volume effects. Measurements were avoided in the areas of void signal at the interfaces between the fat-dominant and water-dominant tissues (India ink artifact).[4] We also avoided measurements in cystic or necrotic components on the T2-weighted images (with and without fat suppression). In the chest wall muscle, we avoided measurements in fat strips.

The CSR was determined by comparing the SI of the thymus gland (tSI) with that of the paraspinal muscle (mSI) on both in-phase (in) and opposed-phase (op) images. The CSR was calculated by using the following equation: CSR = (tSIop/mSIop)/(tSIin/mSIin).[5]

Criteria for thymoma diagnosis based on CT and MRI data. Pirronti et al[6] showed the morphological criteria on CT to differentiate thymoma from hyperplasia. On MRI, in addition to the same morphological criteria used for CT, Priola et al[7] showed the specific MRI criteria for differentiation based on the absence of SI loss on the opposed-phase image relative to the in-phase image. In this study, criteria for the diagnosis of thymoma and nonthymoma are listed in Table 2.

Statistical Analysis

The radiodensity and CSR were expressed as mean values ± standard deviations (all data were normally distributed, based on the Shapiro-Wilk test results); χ^2 test and Fisher exact test were used for comparison of qualitative imaging characteristics between the 2 groups of thymoma and nonthymoma, while *t* test was used for comparison of the radiodensity and CSR between the 2 groups. Logistic multivariate regression was performed by both predictive qualitative and quantitative variables to estimate the probability that patients had thymoma.

The diagnostic ability of radiodensity and CSR for thymoma diagnosis was evaluated using the area under the receiver operating characteristic curve (AUROC). The optimal cutoff points were identified based on Youden index, then were used for calculating the sensitivity (Se), specificity (Sp), and accuracy (Acc) of both CT and MRI. McNemar test was used to compare the diagnostic performance of CT versus MRI. A P value of $<.05$ was considered indicative of a statistically significant difference for all statistical analyses. SPSS 20.0 was used.

Results

Sample Characteristics

A total of 53 patients with MG were included in the statistical analysis. The mean age of men was 40.9 ± 11.6 years, which was not different from that of women (43.9 ± 14.8, P = .43).Of these patients, 45.3% were males and 54.7% were females. Histopathological examination resulted in 33 thymoma and 20 nonthymoma. The mean age of patients with thymoma was significantly higher than that of nonthymoma patients (47.9 ± 11.3 years vs 33.6 ± 11.8 years, $P < .0001$).

Comparison of Imaging Parameters Between Thymoma and Nonthymoma Groups

There was a significant difference between thymoma and nonthymoma groups regarding the counts of imaging qualitative parameters found on CT and MRI. The difference was observed in almost all assessed parameters, except for SI T1-weighted and SI T2-weighted. On both CT and MRI, the most frequent qualitative parameters of thymoma were at lateral position, in mass shape, absence of SI loss on the opposed-phase image relative to the in-phase image, high SI in T2-weighted with fat suppression, and having attenuated soft or mixed tissue. Meanwhile, nonthymoma showed opposite imaging parameters (Table 3).

The mean CSR was higher in the thymoma group than in the nonthymoma group (1.021 ± 0.068 vs 0.648 ± 0.109, $P < .001$; Figure 1A). The mean radiodensity was also higher in the thymoma group than in the nonthymoma group (34.45 ± 21.1 vs −4.65 ± 41.85, $P < .001$; Figure 1B). Despite the significant difference between CT and MRI regarding the frequency of qualitative imaging characteristics (Table 3), logistic regression analyses showed no association between these parameters with the thymoma diagnosis probability, except for CSR at MRI and the shape at CT. The respective odds ratio (95% confidence interval [95% CI]) for CSR and the shape was 8.80 (95% CI: 1.359-56.93) and 11.723 (95% CI: 1.332-103.202), respectively (Table 4).

Differentiating Ability of CSR and Radiodensity in the Diagnosis of Thymoma

The AUROC of CSR and radiodensity in differentiating the 2 groups was 0.981 (95% CI: 0.899-1.000) and 0.798 (95% CI:

Table 3. Qualitative Characteristics of Thymoma and Nonthymoma Patients Based on CT and MR Images.[a]

Characteristic		Thymoma (n = 33)	Non-thymoma (n = 20)	P
Location[b]	Superior	17 (51.5%)	19 (95.0%)	.001[e]
	Inferior	16 (48.5%)	1 (5.0%)	
Position[b]	Middle	10 (30.3%)	15 (75.0%)	.002[e]
	Right, left	23 (69.7%)	5 (25.0%)	
Shape[b]	Gland	3 (9.1%)	15 (75.0%)	<.001[e]
	Mass	30 (90.9%)	5 (25.0%)	
SI loss[c]	Yes	1 (3.0%)	18 (90.0%)	<.001[e]
	No	32 (97.0%)	2 (10.0%)	
SI T1[c]	>Muscle SI, <fat SI	31 (93.9%)	17 (85.0%)	.271[f]
	Other	2 (6.1%)	3 (15.0%)	
SI T2[c]	>Muscle SI, <fat SI	31 (93.9%)	17 (85.0%)	.271[f]
	Other	2 (6.1%)	3 (15.0%)	
SI T2 fat suppression[c]	High	32 (97.0%)	12 (60.0%)	.001[f]
	Low	1 (3.0%)	8 (40.0%)	
Necrosis, cyst[c]	Yes	14 (42.4%)	0 (0.0%)	<.001[e]
	No	19 (57.6%)	20 (100.0%)	
Necrosis, cyst[d]	Yes	10 (30.3%)	0 (0.0%)	<.001[e]
	No	23 (69.7%)	20 (100.0%)	
Attenuation[d]	Fat	1 (3.0%)	8 (40.0%)	.001[e]
	Soft tissue or mixed	32 (97.0%)	12 (60.0%)	

Abbreviations: CT, computed tomography; MR, magnetic resonance; SI, signal intensity.
[a]n = 53.
[b]On both MRI and CT.
[c]On MRI.
[d]On CT.
[e]*P* value from χ^2 test.
[f]*P* value from Fisher exact test.

0.666-0.896), respectively ($P < .05$). Using the cutoff value >0.75, the CSR produced an Se of 100% and an Sp of 95%. Meanwhile, the Se and Sp of radiodensity were 90.9% and 70.0%, respectively (using cutoff value of >18). When combining both qualitative and quantitative parameters, the Acc in thymoma diagnosis of CSR was significantly higher than that of radiodensity, $P = .031$ (Table 5).

Discussion

Qualitative Assessment

Generally, CT is the first choice modality for discriminating between thymomas and thymic lymphoid hyperplasia. On CT, thymomas usually present as sharply demarcated round or oval soft tissue masses in the anterior mediastinum compartment.[8] This typical appearance is highly suggestive of the diagnosis. However, many hyperplasia cases presented with large soft tissue masses, which were easily detected on chest radiograph, were found misdiagnosed as thymoma.[9-13] In patients with MG, Nicolaou et al[14] found thymic lymphoid hyperplasia can exhibit variable morphologies and sizes as it may appear normal (45% of cases), triangular-shaped diffusely enlargement with smooth margin (35%), or as a focal thymic mass (20%). This mass could not be differentiated with thymoma (Figure 2). Pirronti et al found that in patients with MG, CT is a sensitive, specific, and efficient modality for detecting thymoma but is less so for detecting thymic hyperplasia. In Pirronti et al's study, the Se of CT for detecting hyperplasia was only 36%.[6] For MRI, since 1987, Batra et al demonstrated that MRI examination added no clinically important information to results obtained by CT in patients with MG.[15] However, at that time, MRI protocol included only T1-weighted and T2-weighted sequences. With technical development, chemical shift MRI was introduced and used for the discrimination of thymoma from nonthymoma abnormalities not only based on morphologic assessments but also based on finding microscopic fat in soft tissue. Today, chemical shift is the first choice in MRI protocol to evaluate thymic lesion.[16] The normal thymus and hyperplasia contains various amounts of fat tissue, depending on age, with nearly 20% in the first decade of life and increases to reach 40% in the second decade. Chemical shift imaging is much more sensitive to detect this fat by showing the SI loss in the opposed-phase image relative to the in-phase image.[17] Conversely, thymomas have no fat and lack of SI loss. In the general radiology practice, visual assessment of the SI loss is a commonly used method to characterize thymoma as well as adrenal adenoma and liver steatosis. Nevertheless, using visual analysis, the SI loss is not always obvious in tissues containing microscopic fat and should be performed with quantitative assessments.[18] In this study, only 2 hyperplasia cases had no SI loss at visual assessment. One small thymoma embedded in triangular-shaped fatty infiltrated thymus was also not detected. Such high reliability of chemical shift MRI in detecting fat in tissue and discriminating thymoma from nonthymoma in this study is similar to that of several studies.[5,7,19]

Quantitative Assessment

The advantage of quantitative assessment is to use a threshold value for differentiating the lesions. At CT, the optimal cutoff point of 18 HU was used to differentiate thymoma from nonthymoma with Se, Sp, and Acc of 90.9%, 70%, 83%, respectively. However, the AUROC of 0.798 was moderate; in addition, the logistic multivariate regression showed that only shape on CT was significant for distinguishing the 2 groups. Priola et al showed that only shape and unenhanced CT attenuation were significant for discrimination between groups, with probability of 2% and 7.3% of being normal thymus or thymic hyperplasia if the findings had focal shape and heterogeneous attenuation at unenhanced CT, respectively.[7] De Kraker et al found that the evaluation by CT is a highly subjective process. Experience has been reported as an important influencing factor in observation errors.[20]

The SI loss can be assessed qualitatively by direct observation and can be assessed quantitatively by calculating the index of CSR or SI index (SII). Many studies have shown that quantitative assessment is more accurate than qualitative one. For adrenal adenomas, Israel et al have reported such discordance

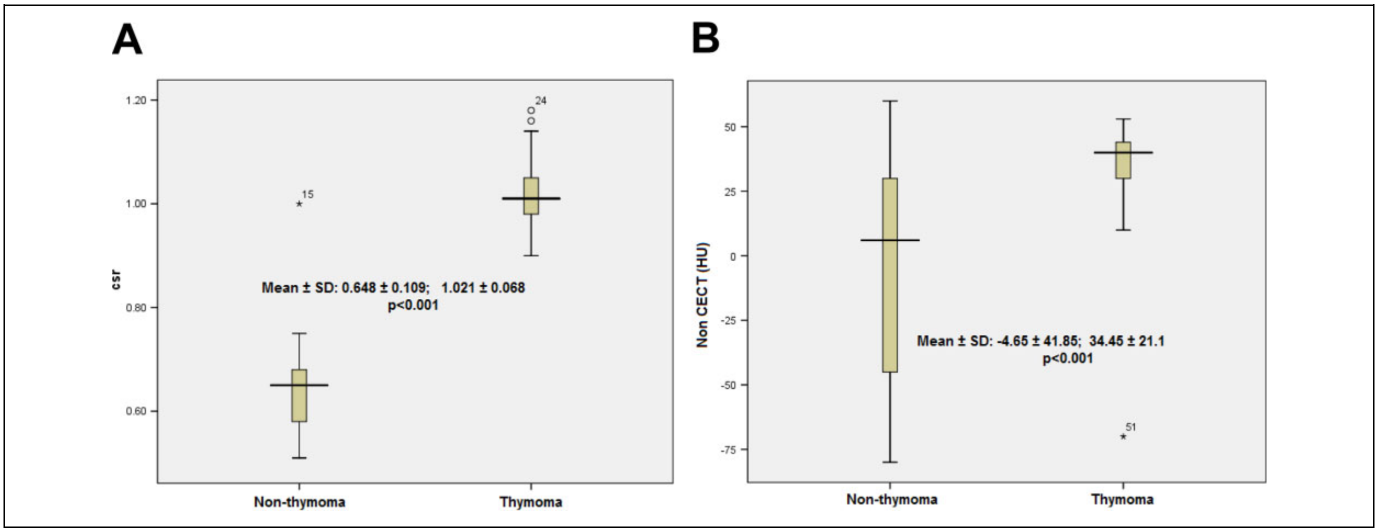

Figure 1. Box-and-whisker plots show the CSR (A) and radiodensity (in HU) (B) values for all cases in the thymoma and nonthymoma groups. The boxes represent data from the 25th to the 75th percentile. The horizontal line inside the boxes is the median value. The vertical lines and whiskers indicate 10th and 90th percentiles. The values outside this range are displayed as individual point. *P* value from *t* test. CSR indicates chemical shift ratio; non-CECT, noncontrast enhancement computed tomography.

Table 4. Odds Ratio and Associated 95% Confident Intervals of Thymoma Diagnostic Probability According to Imaging Parameters.

	MRI		CT	
Qualitative parameter	OR	95% CI	OR	95% CI
Shape (gland vs mass)	41.43	0.07-2542.00	11.72	1.33-103.20
Location (superior vs inferior)	10.11	0.00-536.00	-	-
Position (middle vs right, left)	1.15	0.00-334.49	3.69	0.70-19.46
Necrosis, cyst (no vs yes)	-	-	-	-
SI T2 fat suppression (low vs high)	-	-	-	-
SI loss (yes vs no)	-	-	-	-
CSR (per 0.1)	8.80	1.36-56.93	-	-
Attenuation (fat soft tissue, mixed)	-	-	1.73	0.66-4.50
Radiodensity (per 10 HU)	-	-	1.07	0.82-1.40

Abbreviations: CI, confidence interval; CSR, chemical shift ratio; CT, computed tomography; MRI, magnetic resonance imaging; OR, odds ratio; SI, signal intensity.

Table 5. Ability of Qualitative, Quantitative, and Both Analyses for MRI in Differentiating Thymoma and Nonthymoma Groups.[a]

Technique	Sensitivity, % (n)	*P*	Specificity, % (n)	*P*	Accuracy, % (n)	*P*
Qualitative						
CT	93.9 (31/33)	1.00	65.0 (13/20)	.062	83.0 (44/53)	.031
MRI	97.0 (32/33)		90.0 (18/20)		94.3 (50/53)	
Quantitative						
CT	90.9 (30/33)	.25	70.0 (14/20)	.062	83.0 (44/53)	.008
MRI	100.0 (33/33)		95.0 (19/20)		98.1 (52/53)	
Both						
CT	93.9 (31/33)	.50	75.0 (15/20)	.125	86.8 (46/53)	.031
MRI	100.0 (33/33)		95.0 (19/20)		98.1 (52/53)	

Abbreviations: CT, computed tomography; MRI, magnetic resonance imaging.
[a]*P* value from McNemar test.

in 7% (3 of 42) of cases in which the quantitative parameters have characterized a lipid-rich adenoma (CSR = 0.41-0.67 and SII = 36%-58%), but the qualitative analysis did not yield SI loss.[21] Park et al also found the SI loss directly be observed was not sensitive than CSR measurement.[22] In addition, for the assessment of hepatic steatosis, the studies have reported a lipid

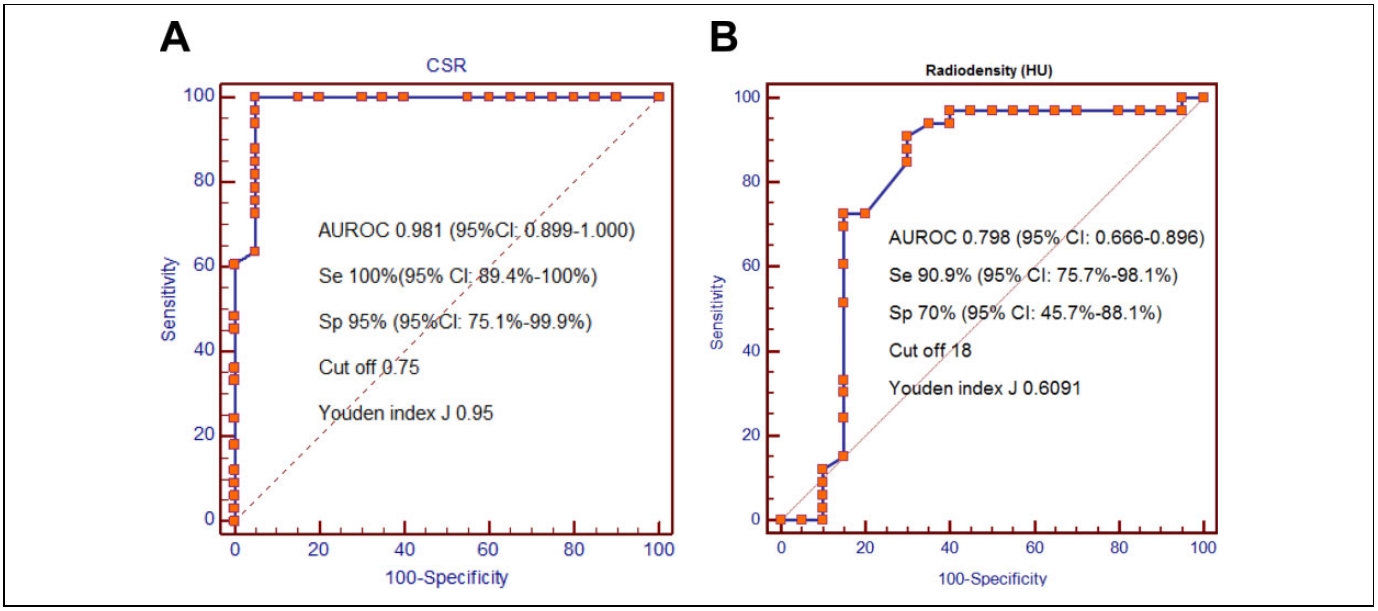

Figure 2. The ROC curves indicate the sensitivity, specificity, and optimal cutoff value of CSR (A) and radiodensity-based (B) differentiation in thymoma and nonthymoma groups. CSR indicates chemical shift ratio; ROC, receiver operating curve.

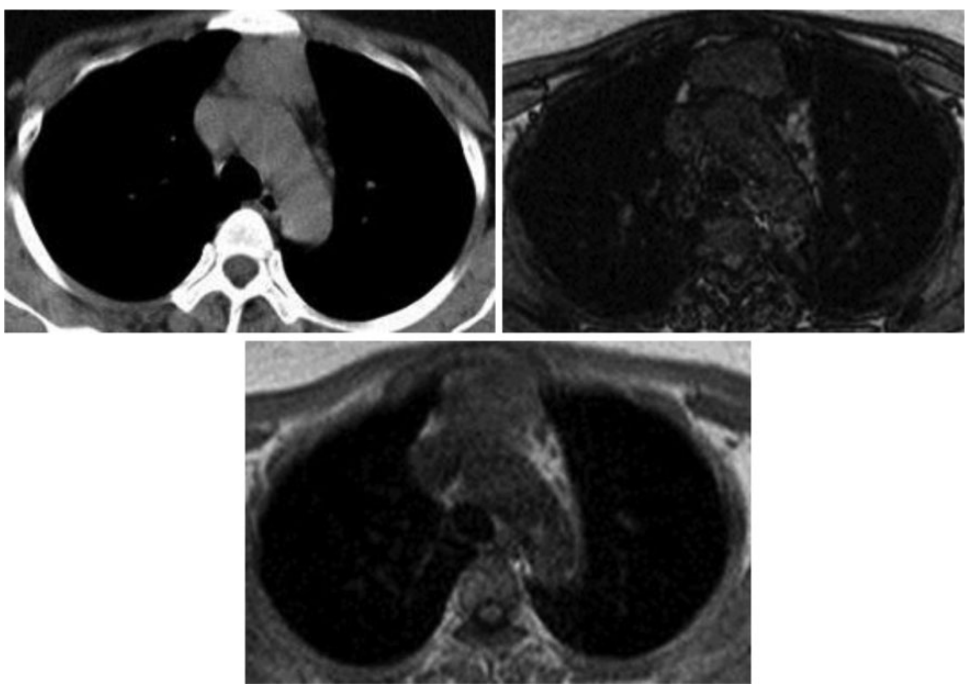

Figure 3. A 21-year-old woman with TLH. The CT findings showed the large mass with density of soft tissue (40 HU). Chemical shift MRI demonstrated no signal intensity loss on the opposed-phase images relative to the in-phase images, suggesting the absence of fat component. The CSR was 0.68. CSR indicates chemical shift ratio; CT, computed tomography; MRI, magnetic resonance imaging; TLH, thymic lymphoid hyperplasia.

concentration threshold greater than 10% or 15% for detecting SI loss on the opposed-phase image relative to the in-phase image at visual assessment.[23,24] Priola et al have reported 2 hyperplasia cases with the absence of SI loss, but SII was 7.8% and 12.7%, respectively.[18] In this study, CSR was an important, independent criterion for differentiating thymoma from nonthymoma with an AUROC of 0.981. With the optimal cutoff point 0.75, CSR had the Se, the Sp, and the Acc of 100%, 95%, and 98.1%, respectively. In addition, although many signs differed significantly between the 2 groups, the logistic

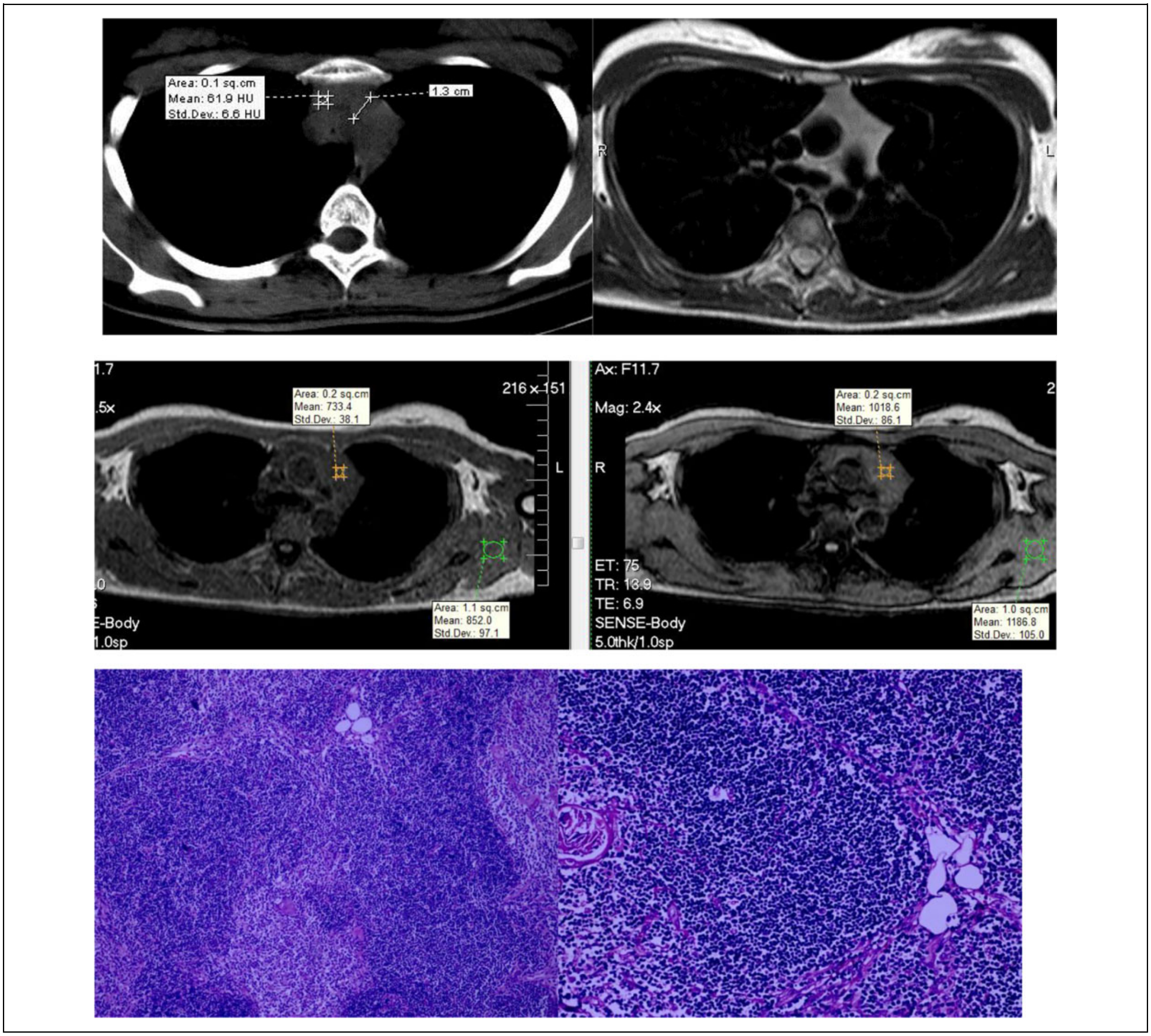

Figure 4. A 22-year-old woman with TLH. Both CT and MRI showed a bilobed shaped soft tissue homogeneous gland with straight margins without the signal intensity loss in the opposed-phase image relative to the in-phase image. The CSR value was 1.0. A histopathologic image exhibits preserved architecture of the thymus, consisting of cortex, medulla, and Hassall corpuscles with lymphoid follicles and minimally fatty infiltrated thymic tissue. CSR indicates chemical shift ratio; CT, computed tomography; MRI, magnetic resonance imaging; TLH, thymic lymphoid hyperplasia.

multivariate regression showed only CSR was significant for differentiation between thymoma and nonthymoma. One hyperplasia case with absence of SI loss was correctly interpreted by CSR 0.68 (Figure 3). Only 1 hyperplasia case, a 22-year-old woman (Figure 4), with absence of SI loss and CSR 1.0 was misdiagnosed in this study. In this case, postoperative histopathological findings showed only a few fat cells, which was not sufficient to detect the SI loss on chemical shift MRI. Some normal or hyperplasia cases with no SI loss have been recently reported in the literature.[3,25,26] With thymic hyperplasia cases without fat (Figure 5), Priola suggested that diffusion-weighted MRI could be valuable by demonstrating restricted diffusion and low apparent diffusion coefficient (ADC) values. His study showed with the cutoff ADC of 1.625×10^{-3} mm^2/s, diffusion-weighted MRI could differentiate thymic tumor from nonthymic lesions with Se 96.8% and Sp 79.2%.[27] However, until now this has been the only study using diffusion-weighted MRI to distinguish thymic tumor from normal and hyperplasia thymus. Studies of Ahmed Abdel Khalek,[28] Razek et al,[29] Usuda et al,[30] Seki et al,[31] and

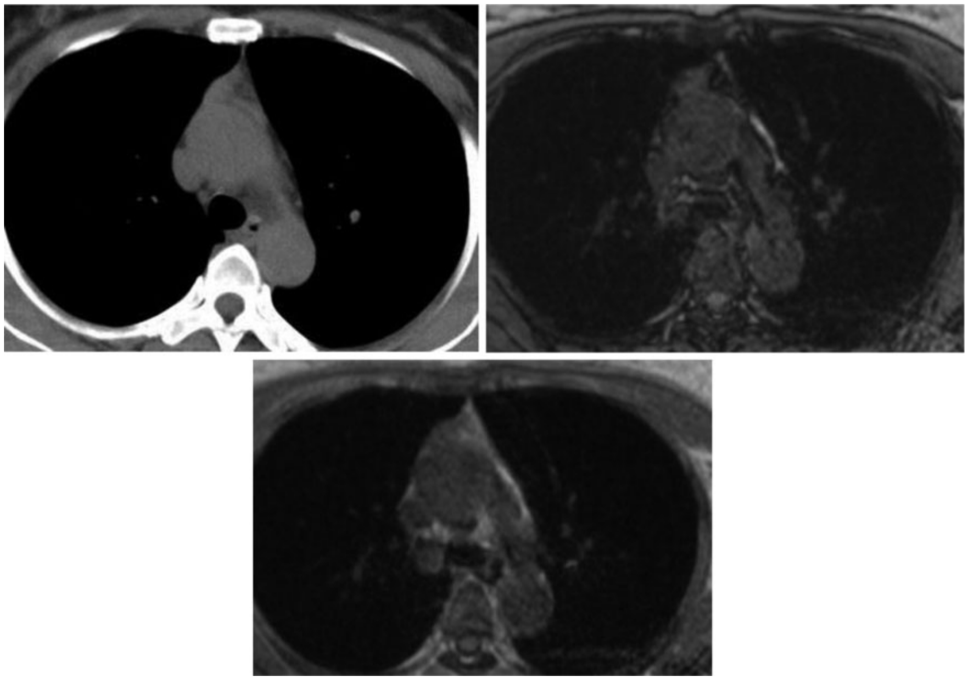

Figure 5. A 49-year-old woman with thymoma. The CT findings showed the heterogeneous bilobulate gland with mixed soft tissue and fat density (−20 to 30 HU). Chemical shift MRI demonstrated no signal intensity loss on the opposed-phase images relative to the in-phase images. The CSR was 0.92. CSR indicates chemical shift ratio; CT, computed tomography; MRI, magnetic resonance imaging.

Gumustas et al[32] often use diffusion-weighted MRI to distinguish benign versus malignant tumors. Therefore, the matter should be further studied.

Magnetic resonance imaging is not the favored modality of choice for the assessment of thymic abnormalities. Usually, CT is the first choice. After detecting a mass anterior to the compartment, diagnosticians could use PET-CT to differentiate thymic neoplasm from normal and hyperplastic tissues. Neoplasm manifests increased metabolic activity with high standard uptake value (SUV) value. PET-CT used to be considered as a highly sensitive and specific imaging technique, especially for patients with lymphoma. However, the studies show that the increased fluorodeoxyglucose uptake could be found in normal, thymic lymphoid hyperplasia or rebound thymic hyperplasia.[2,33,34] Due to the overlap of the SUV of neoplasm with non-neoplasm, SUV value cannot reliably distinguish between these lesions.[35] In this setting, chemical shift MRI could be helpful to distinguish neoplasm from non-neoplasm based on threshold value of CSR.

Although SII can be used for the quantification of fat tissue, especially in dual-echo technique, the use of this index is not as common as the CSR. This may be because the reference tissue may contain determined amount of fat and therefore may be incorrect.[17] In a study of Priola,[18] SII had both Se and Sp of 100% (at cutoff point 8.92), while CSR had the respective Se 100% and Sp 96.7% (at cutoff point 0.85). No overlap in SII values was found between the 2 groups, while CSR values overlapped in some cases. However, this difference was negligible.[3] Both Inaoka[5] and Popa et al[19] used CSR for studying despite one with non-dual-echo technique and one with dual-echo. In our study, CST was applied because the non-dual-echo technique was used in four cases.

Despite strengths in study design, the findings of the present study should be interpreted with some precaution. This is because only patients who underwent surgery were included and the present findings may not be generalizable to wider population with MG. In addition, non-dual-echo techniques were performed in 4 patients. Because of the in-phase and opposed-phase images obtained in different times from 2 radiofrequency excitations, the misregistration could mislead the observation of SI loss.

Conclusion

Chemical shift MRI was more accurate than CT and more helpful for differentiating thymoma from nonthymoma in patients with MG.

Authors' Note

The present study was approved by the Ethical Review Committee of Hanoi Medical University (No 164B/HĐĐĐĐHYHN, December 10, 2014). All participants provided written consent forms.

Acknowledgments

The authors are grateful to the study participants. The authors also thank the medical and nursing staff of the participating hospitals for their assistance in patient recruitment.

Declaration of Conflicting Interests

The author(s) declared no potential conflicts of interest with respect to the research, authorship, and/or publication of this article.

Funding

The author(s) received no financial support for the research, authorship, and/or publication of this article.

References

1. Onodera H. The role of the thymus in the pathogenesis of myasthenia gravis. *Tohoku J Exp Med*. 2005;207(2):87-98.
2. Priola AM, Priola SM. Imaging of thymus in myasthenia gravis: from thymic hyperplasia to thymic tumor. *Clin Radiol*. 2014; 69(5):e230-e245.
3. Phung T, Nguyen T, Tran D, Phan N, Nguyen H. A thymic hyperplasia case without suppressing on chemical shift magnetic resonance imaging. *Case reports in radiology*. 2018;2018: 73056194.
4. Priola AM, Priola SM, Ciccone G, et al. Differentiation of rebound and lymphoid thymic hyperplasia from anterior mediastinal tumors with dual-echo chemical-shift MR imaging in adulthood: reliability of the chemical shift ratio and signal intensity index. *Radiology*. 2015;274(1):238-249.
5. Inaoka T, Takahashi K, Mineta M, et al. Thymic hyperplasia and thymus gland tumors: differentiation with chemical shift MR imaging. *Radiology*. 2007;243(3):869-876.
6. Pirronti T, Rinaldi P, Batocchhi AP, Evoli A, Schino CD, Marano P. Thymic lesions and myasthenia gravis: diagnosis based on mediastinal imaging and pathological findings. *Acta Radiol*. 2002;43(4):380-384.
7. Priola AM, Priola SM, Gned D, Giraudo MT, Fornari A, Veltri A. Comparison of CT and chemical-shift MRI for differentiating thymoma from non-thymomatous conditions in myasthenia gravis: value of qualitative and quantitative assessment. *Clin Radiol*. 2016;71(3):e157-e169.
8. Takahashi K, Al-Janabi NJ. Computed tomography and magnetic resonance imaging of mediastinal tumors. *J Magn Reson Imaging*. 2010;32(6):1325-1339.
9. Danilovic DLS, Martin RM, Caruso P, Marui S. Thymic hyperplasia in Graves' disease. *Clinics (Sao Paulo)*. 2011;66(12): 2177-2178.
10. Mizuno T, Hashimoto T, Masaoka A, Andoh S. Thymic follicular hyperplasia manifested as an anterior mediastinal mass. *Surgery Today*. 1997;27(3):275-277.
11. Heiser RN, Bogar WC, Cambron J, Fergus MP. Thymic follicular hyperplasia presenting as a large mediastinal mass in a 42-year-old woman. *Clinal Pulmonary Medicine*. 2009;16(4): 229-231.
12. Nakagawa M, Hara M, Itoh M, Shibamoto Y. Nodular thymic lymphoid follicular hyperplasia mimicking thymoma. *Clin Imaging*. 2008;32(1):54-57.
13. Hamzaoui AA, Klii RR, Salem RR, Kochtali I, Golli MM, Mahjoub SS. Thymic hyperplasia in a patient with Grave's disease. *Int Arch Med*. 2012;5:6.
14. Nicolaou S, Muller NL, Li DKB, Oger JJF. Thymus in myasthenia gravis: comparison of CT and pathologic findings and clinical outcome after thymectomy. *Radiology*. 1996;201(2):471-474.
15. Batra P, Herrmann C, Mulder D. Mediastinal imaging in Myasthenia Gravis: correlation of chest radiography, CT, MR, and surgical finding. *AJR Am J Roentgenol*. 1987;148(3): 515-519.
16. Daye D, Ackman JB. Characterization of mediastinal masses by MRI: techniques and applications. *Applied radiology*.2017;46(7): 10-22.
17. Hood MN, Ho VB, Smirniotopoulos JG, Szumowski J. Chemical shift the artifact and clinical tool revisited. *Radio Graphics* 1999; 19(2):357-371.
18. Priola AM, Gned D, Veltri A, Priola SM. Chemical shift and diffusion-weighted magnetic resonance imaging of the anterior mediastinum in oncology: current clinical applications in qualitative and quantitative assessment. *Crit Rev Oncol Hematol.* 2016;98:335-357
19. Popa G, Preda EM, Scheau C, Lupescu IG. Updates in MRI characterization of the thymus in myasthenia patients. *J Med Life*. 2012;5(2):206-210.
20. De Kraker M, Kluin J, Renken N, Maat AP, Bogers AJ. CT and myasthenia gravis: correlation between mediastinal imaging and histopathological findings. *Interact Cardiovasc Thorac Surg*. 2005;4(3):267-271.
21. Israel GM, Korobkin M, Wang C, Hecht EN, Krinsky GA. Comparison of unenhanced CT and chemical shift MRI in evaluating lipid-rich adrenal adenomas. *AJR Am J Roentgenol*. 2004;183(1): 215-219.
22. Park BK, Kim CK, Kim B, Lee JH. Comparison of delayed enhanced CT and chemical shift MR for evaluating hyperattenuating incidental adrenal masses. *Radiology*. 2007;243(3): 760-765.
23. Lee SS, Lee Y, Kim N, et al. Hepatic fat quantification using chemical shift MR imaging and MR spectroscopy in the presence of hepatic iron deposition: validation in phantoms and in patients with chronic liver disease. *J Magn Reson Imaging*. 2011;33(6): 1390-1398.
24. Hussain HK, Chenevert TL, Londy FJ, et al. Hepatic fat fraction: MR imaging for quantitative measurement and display early experience. *Radiology*. 2005;237(3):1048-1055.
25. Ackman JB, Mino-Kenudson M, Morse CR. Nonsuppressing normal thymus on chemical shift magnetic resonance imaging in a young woman. *J Thorac Imaging*. 2012;27(6):196-198.
26. Priola AM, Gned D, Marci V, Veltri A, Priola SM. Diffusion-weighted MRI in a case of nonsuppressing rebound thymic hyperplasia on chemical-shift MRI. *Jpn J Radiol*. 2015;33(3):158-163.
27. Massimiliano PA, Massimo PS, Teresa GM, et al. Chemical-Shift and Diffusion-Weighted magnetic resonance imaging of thymus in myasthenia gravis: usefulness of quantitative assessment. *Invest Radiol*. 2015;50(4):228-238.
28. Khalek AA, Mansoura EG. Characterization of thymic tumors with diffusion weighted MR imaging. Paper presented at: European Society of Radiology; Europe, 2010.
29. Razek AAKA, Khairy M, Nada N. Diffusion-weighted MR imaging in thymic epithelial tumors: correlation with World Health

Organization Classification and Clinical Staging. *Radiology*. 2014;273(1):268-275.
30. Usuda K, Maeda S, Motono N, et al. Diffusion weighted imaging can distinguish benign from malignant mediastinal tumors and mass lesions: comparison with positron emission tomography. *Asian Pac J Cancer Prev*. 2015;16(15):6469-6475.
31. Seki S, Koyama H, Ohno Y, et al. Diffusion-weighted MR imaging vs multi-detector row CT: direct comparison of capability for assessment of management needs for anterior mediastinal solitary tumors. *Eur J Radiol*. 2014;83(5):835-842.
32. Gumustas S, Inan N, Sarisoy HT, et al. Malignant versus benign mediastinal lesions: quantitative assessment with diffusion weighted MR imaging. *Eur Radiol*. 2011;21(11):2255-2560.
33. Priola AM, Galetto G, Priola SM. Diagnostic and functional imaging of thymic and mediastinal involvement in lymphoproliferative disorders. *Clin Imaging*. 2014;38(6):771-784.
34. Ferdinand B, Gupta P, Kramer EL. Spectrum of thymic uptake at ^{18}F-FDG PET. *RadioGraphics*. 2004;24(6):1611-1616.
35. Kulkarni NM, Pinho DF, Narayanan S, Kambadakone AR, Abramson JS, Sahani DV. Imaging for oncologic response assessment in lymphoma. *AJR Am J Roentgenol*. 2017;208(1):18-31.